PCCP

COMMUNICATION

View Article Online
View Journal

Cite this: DOI: 10.1039/c8cp05465g

Received 29th August 2018,
Accepted 4th October 2018

DOI: 10.1039/c8cp05465g

rsc.li/pccp

Near interface ionic transport in oxygen vacancy stabilized cubic zirconium oxide thin films†

Mohsin Raza, *[ab] Simone Sanna,[a] Lucia dos Santos Gómez,[ac] Eric Gautron,[d] Abdel Aziz El Mel,[d] Nini Pryds,[a] Rony Snyders,[be] Stéphanos Konstantinidis[b] and Vincenzo Esposito *[a]

Published on 04 October 2018. Downloaded by DTU Library on 10/11/2018 11:25:52 AM.

The cubic phase of pure zirconia (ZrO_2) is stabilized in dense thin films through a controlled introduction of oxygen vacancies (O defects) by cold-plasma-based sputtering deposition. Here, we show that the cubic crystals present at the film/substrate interface near-region exhibit fast ionic transport, which is superior to what is obtained with similar yttrium-stabilized cubic zirconia thin films.

Oxygen defective metal oxides (MeOs) hold a prominent role in the renewable energy technologies as they are used as ionic conductor/electrolyte in energy storage and conversion devices.[1–3] Over the last decade the interest in such functional materials has further increased significantly as they possess a high potential in a vast range of information and communication applications, *e.g.*, memristors[4] and microelectromechanical systems (MEMS).[5] This is the case of ionotronics, where tuneable electronic properties raise from defects created in the ionic structures electrochemically *via* the activation of multiple charge compensation mechanisms.[6,7] In oxide ionic conductors, oxygen vacancies are generally created by incorporating aliovalent dopants, such as in yttrium-stabilized zirconia (YSZ).[5,8] However, there are several other ways to control or influence their properties, *e.g.* by dealing at nano-scale and creating interfaces, where defects can be confined in strained lattices and electrostatic polarized regions.[9–13] In past years, enhanced oxygen ionic conductivity in many MeOs, *e.g.*, BiVCuO, CeGdO, LaSrGaMgO, YSZ, have been investigated.[14] Among those, stabilized cubic zirconium dioxide or cubic fluorite zirconia is surely the most used and reliable ionic conductor.

Ionic conductivity in zirconia is due to the mobility of O vacancies in the fluorite lattice. Such charges are enhanced by the solubilization of aliovalent dopants, *e.g.* yttrium (Y^{3+}), in the zirconia (ZrO_2) that also stabilizes the most conductive cubic fluorite form. As at first it was found that the ionic conductivity in oxides is proportional to the number of O vacancies present in the material, it was expected that the ionic conductivity increases with increasing of O vacancy concentration, *i.e.* extrinsically, by increasing the dopant content. However, the maximum ionic conductivity in yttria-stabilized zirconia (YSZ) has been found for 7–9 mol% Y_2O_3 at 327–1227 °C.[15,16] The incorporation of higher amounts of dopants in YSZ actually lowers the O vacancies mobility, as in YSZ the migration energy across the Y–Y common edge is higher as compared to the diffusion across the Zr–Y common edge.[15] To enhance the ionic conductivity at lower temperatures, other pathways to stabilize cubic zirconia at room temperature have been thus suggested. The stabilization mechanism of cubic zirconia without any dopants *i.e.* just incorporating O vacancies in the zirconia matrix theoretically was proposed by Fabris *et al.*[17] Recently, Raza *et al.*,[18] combining computational and experimental studies, demonstrated that the cubic zirconia can indeed be stabilized at room temperature without any dopants, just by incorporating oxygen vacancies in the zirconia lattice. By using density functional theory (DFT) calculations on multiple O vacancies containing arrangements (randomly distributed and clustered), Raza *et al.*[18] also showed that the cubic phase is the most thermodynamically stable phase as compared to the monoclinic and tetragonal phases, when the concentration of O vacancies is low as 3 at%. The same behaviour for forming cubic zirconia was found unambiguously for zirconia films, where it is synthesized with 3 at% O vacancies using DC magnetron sputtering.[18] In such deposition process, oxygen-vacancy stabilized cubic zirconia (OVSZ) was found to form below a film thickness of 850 nm. Above 850 nm, the low temperature monoclinic phase appears. Such a variety of phases in the same deposition suggests that some form of metastability, relative to defective features of are introduced at structural and/or microstructural levels during the

[a] *Department of Energy Conversion and Storage, Technical University of Denmark, DTU Risø Campus, DK-4000 Roskilde, Denmark. E-mail: vies@dtu.dk*
[b] *Chimie des Interactions Plasma-Surface (ChIPS), University of Mons, 23 Place du Parc, 7000 Mons, Belgium. E-mail: mohsinraza.khan@outlook.com*
[c] *Depto. Química Inorgánica, Cristalografía y Mineralogía Facultad de Ciencias, Universidad de Málaga Campus de Teatinos s/n, 29071 Malaga, Spain*
[d] *Institut des Matériaux Jean Rouxel (IMN), Université de Nantes, CNRS, 2 rue de la Houssinière, BP 32229, 44322 Nantes cedex 3, France*
[e] *Materia Nova Research Center, Parc Initialis, B-7000 Mons, Belgium*
† Electronic supplementary information (ESI) available. See DOI: 10.1039/c8cp05465g

View Article Online

Published on 04 October 2018. Downloaded by DTU Library on 10/11/2018 11:25:52 AM.

condensation of the film.[19–21] Due to the stability of the different phases in zirconia, a natural equilibration towards stable phases is expected at high temperatures, where ionic conductivity is activated, since the oxygen defects are mobile and spontaneously equilibrated with the oxygen gas in the atmosphere. Moreover, ionic conductivity is also expected to be low, where a large amount of O vacancies are incorporated in the OVSZ.

In the present work, we studied the microstructural and electrical properties of OVSZ, considering both the influence of the oxygen vacancies incorporated at the deposition step, the effect of the film-substrate interface and the nanometric scale of the microstructure in the film. Cubic-phase OVSZ thin films containing 3 and 16 atomic% of O vacancies are deposited with thicknesses varying from 10 to 2000 nm on several different substrates, *i.e.* Si(100), Si/SiO (passivated silicon), $NdGaO_3$ (NGO) and borosilicate glass. The films were prepared using dc-reactive magnetron sputtering (dc-RMS), working inside the so-called transition zone.[18] Transition zone is a highly sensitive region in the dc-reactive magnetron sputtering where under-stoichiometric films of various chemical content can be deposited using a feedback control unit. More details on OVSZ thin film deposition, determination of the vacancy concentration, characterization and c-phase stabilization can be found in Fig. S1 (ESI†) and ref. 18. For the evaluation of the crystal structure in the present study, XRD in the grazing incidence configuration (GIXRD) and electron diffraction (ED) performed in a transmission electron microscope (TEM) are used. To investigate the film morphology, scanning electron microscope (SEM) cross-sectional images and high resolution TEM (HR-TEM) analysis are performed. SEM observations (Fig. S2, ESI†) report morphological characterization in a larger scale, indicating the presence of a columnar-like growth with branched feather-like formations with an inter-columnar porosity. They also indicated the presence of a near substrate/film interface dense polycrystalline region of a *ca.* 200 nm (further details shown in the ESI,† Fig. S2). Fig. 1 shows typical features in details by cross-section of the thin film using HR-TEM of samples deposited on Si/SiO. Fig. 1(a–c) show the overall microstructure for a film of *ca.* 950 nm in thickness deposited on Si. The figures indicate the presence of columnar structure of the films with a variety of different features along its thickness (b and c). A columnar growth is generally expected in thin films deposited at low temperatures by PVD and our experiments also show that these features are nearly identical features in the films deposited on other substrates. High magnification micrographs at the core and the top-surface of the film (b and c) show a rather disordered clustering of the crystallites, which further grow in a long-range hierarchical feather-like microstructure and indicate the presence of aligned porosity along the columns. However, this porosity is not detected in the near substrate/film interface (see details in Fig. S3, ESI†). For the structure, local electron diffraction patterns and FFT performed respectively on the whole film show that a stable monoclinic phase is detected only above 850 nm thick film at the edge of the columns (Fig. S4 (c) and (d), ESI†). On the other hand near the porosity indicate that the columns have a cubic structure (complete characterization in Fig. S4, ESI†). While for the thick film a mixture of phases is registered, for the thin film the cubic crystals is dominant in the near substrate/film interface region. Fig. 1(e–h) shows HR-TREM observations at a 150 nm thin film, made to represent the substrate/film interface region. Crystallites in Fig. 1(f and g) resulted in the range of *ca.* 5 nm throughout the whole thickness, with no evidences of porosity. Stabilization of tetragonal/cubic phases of zirconia at room temperature is generally attributed to the grain size effects.[22] However, it has been also shown that below a critical crystal size (5–50 nm), oxygen ion vacancies are crucial in the lattice strain.[23] The presence of cubic phase with multiple orientation and with a slight dominance of (111) and (100) plane is revealed by ED pattern in Fig. 1(h). This result is representative of the whole 150 nm film.

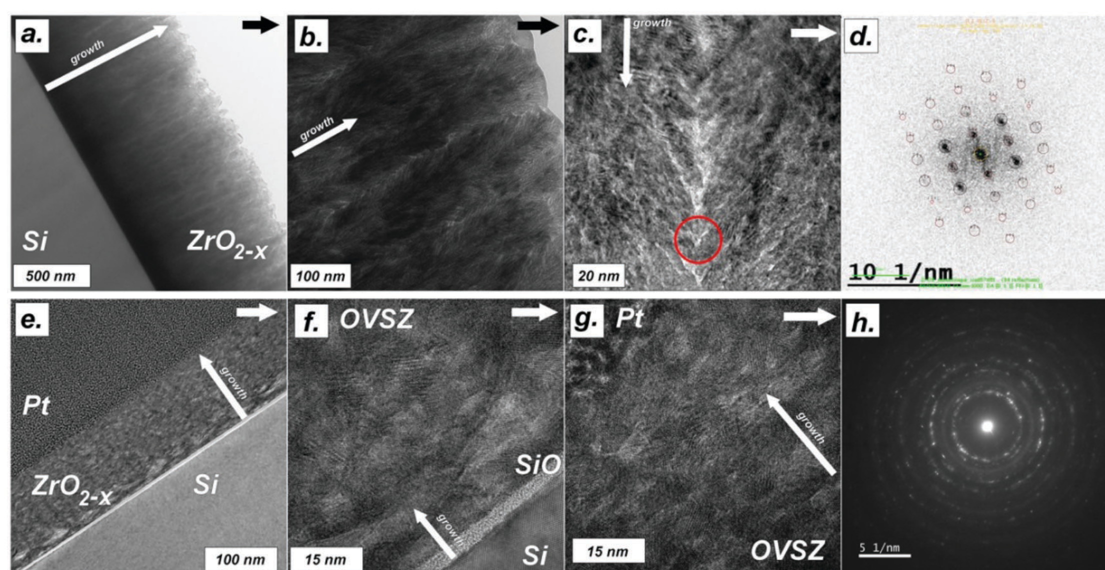

Fig. 1 HR-TEM pictures of the ZrO_{2-x} thin film deposited on Si–SiOx substrate by reactive dc-magnetron sputtering at room temperature showing the overall microstructures (a, e), different morphologies and electron diffraction signal FTT for a 950 nm (a–f) and 150 nm (e–h) thin samples.

This journal is © the Owner Societies 2018

Published on 04 October 2018. Downloaded by DTU Library on 10/11/2018 11:25:52 AM.

An overall crystallography analysis of samples with different thicknesses and on different substrates (Si/SiO and NGO) is carried out by GIXRD. Detailed characterization is reported in the ESI,† showing representative examples of diffraction on OVSZ films, *i.e.* with 16 atomic% O vacancies on Si/SiO and NGO (Fig. S5, ESI†). The overall diffraction results are consistent with HR-TEM analysis and indicate a clear prevalence of the cubic phase for low film thicknesses below of *ca.* 200 nm. The distinction of tetragonal *vs.* cubic phase is resolved as reported in ref. 18. Moreover, it is also found that the substrate type did not influence the plane orientation, *i.e.* (111) remained dominant for all the substrates (see Fig. S4, ESI†). The (111) orientation if the lowest energy in fluorites and, due to the low deposition temperature, the substrates do not influence the growth.[21]

For the electrical properties of the films, both four-probe method and electrochemical impedance spectroscopy (EIS) are performed. Measurements on the films above 500 nm show high in-plane resistance at high temperatures. This is attributed to the inter-columnar aligned porosity that intercepts the electrical current that would flow in the in-plane directions.[24] For the thinner samples, the conductive substrates, *e.g.* Si and glass, impair the measurement, resulting in a high value of the conductivity, even at low temperatures, mainly originated from the substrate. To avoid such an artefact, OVSZ thin films are characterized on NGO single crystal substrates (Crystal Germany). NGO does not contribute to the overall conduction.[13] Since the OVSZ cubic phase is found to be stable up-to 750 °C,[25] EIS measurements are carried out up to 725 °C. To determine the nature of the conductivity, *i.e.* ionic *vs.* electronic conductivity, we use different partial pressure conditions: air, pure nitrogen and in 6% hydrogen-nitrogen mixture (*i.e.* reducing condition).[26] Further details on the electrochemical measurements are reported in other publications.[20]

Fig. 2 shows the EIS characterization: (a) and (b) report the effect of the thickness on conductivity for samples at 3 at% (a) and 16 at% (b) of oxygen vacancies, respectively. The Arrhenius plots indicate that thinner films have higher conductivity with increased activation energy (E_a) at lower thickness, from 1.2 to 1.6 eV. Instability is registered for the 100 nm film at 16 at% only (b) with a change in conductivity at low temperatures. Fig. 2(c) shows a direct comparison of the effect of vacancies content in the film, with respect to nanocrystalline YSZ thin films, as reported by Kosacki.[27] The Arrhenius plot indicates a comparable conductivity of the OVSZ samples, with higher conductivity for the 3 at% samples at 10 nm. Higher conductivity than the YSZ sample is also registered. Higher values of activation energy for the OVSZ samples than for the YSZ reference indicated a certain degree of constrain of the oxygen vacancy mobility for the pure zirconia compared to the Y-doped one. This effect is not expected for "intrinsic" defects. However, the high disorder and the metastable nature of the samples can reasonably lead to a rise of defect hopping energy.[17] This is especially considering that the electrostatic balance between the artificial vacancies and the Zr^{4+} cations is expected to lead to a stronger electrostatic interaction than for Y^{3+}-doped zirconia. Moreover, due to both the higher conductivity of the OVSZ samples and the nanocrystalline microstructures, space charge region effects are expected, especially for the un-doped form.[10,28] To clarify the nature of the conductivity, Brower-like plots, *i.e.* conductivity *vs.* pO_2 plots, are shown in Fig. 3(a and b). These plots indicate that the conductivity pO_2 is independent for the 10 nm samples. Such behaviour suggests that the materials have a dominant ionic conductivity, while no evidences of n-type conductivity, usually related to the formation of polarons, are registered. On the other hand, increased ionic conductivity for the cubic-OVSZ can be attributed to absence of extrinsic dopants, which promotes the apparition of a preferential ionic conductivity path throughout the nanocrystalline phase. Since the samples are dopant free, disordered and condensed at low temperatures, it is assumed that our results emphasize a novel path towards ionic conductivity enhancement. The latter is driven by the interface between the thin film and the substrate. It is also remarkable that, despite the metastable nature, high conductivity persists in a wide range of thicknesses and temperatures. This result, together with the relevance of synthesizing defective metal oxides thin films at low temperatures, has a high importance for those micro- and nano-technologies where low

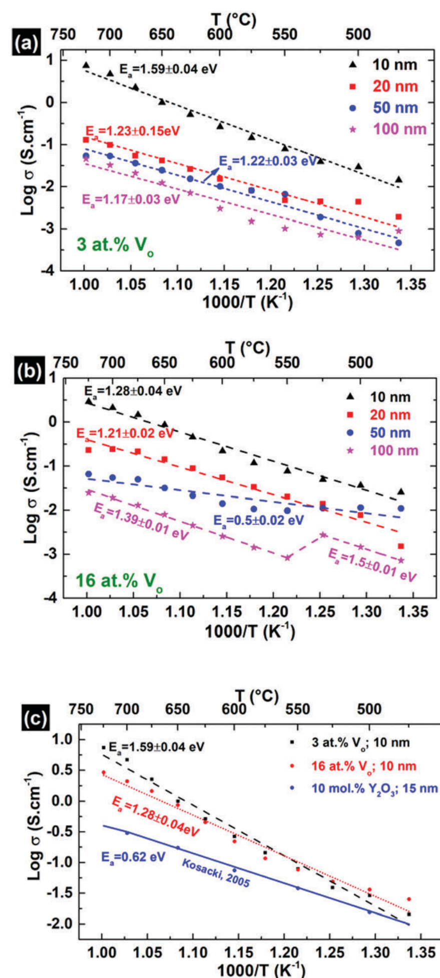

Fig. 2 Electrical properties of OVSZ thin films containing (a) 3 atomic% and (b) 16 atomic% of oxygen vacancies in the structures deposited on NGO (c) comparison of OVSZ thin films with Kosacki *et al.*[27]

View Article Online

Published on 04 October 2018. Downloaded by DTU Library on 10/11/2018 11:25:52 AM.

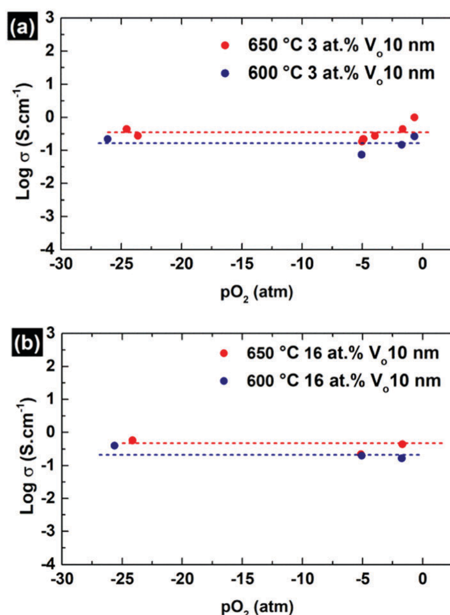

Fig. 3 (a) and (b) shows the electrical properties of 10 nm OVSZ thin films (deposited on NGO) as a function of oxygen partial pressure.

processing temperatures are essential to preserve the thermo-chemo-mechanical integrity of the system, *e.g.* for Si-based MEMS.

Conclusions

Oxygen vacancy stabilized cubic zirconia is synthesized as thin film by reactive dc-sputtering at room temperature. The near substrate-film interface is dense, polycrystalline and characterized by the presence of solely cubic crystals. Oxygen vacancy stabilized cubic zirconia result metastable up to 750 °C, and atmospheres, both oxidative and reducing. These features appear independent of the substrates. Such a region also shows high ionic conductivity, achieving typical values above 3 S cm^{-1} at 700 °C for 10 nm thin films, and typical activation energies above 1.2 eV. Remarkably, such conductivity is around one order of magnitude larger than reached by polycrystalline YSZ thin films with similar features. Measurements of conductivity in reactive gas atmospheres highlight the presence of dominating oxygen ion conductivity.

Conflicts of interest

There are no conflicts to declare.

Acknowledgements

This work is partially supported by the Belgian Government through the "Pôle d'Attraction Inter universitaire" (PAI, "Plasma-Surface Interaction", Ψ). S. Konstantinidis is research associate of the National Fund for Scientific Research of Belgium (FNRS) and Danish Council for Independent Research|Technology and Production Sciences for the Project 2 (grant no. 48293) which supported V. Esposito.

References

1 S. M. Haile, *Acta Mater.*, 2003, **51**, 5981–6000.
2 V. V. Kharton, F. M. B. Marques and A. Atkinson, *Solid State Ionics*, 2004, **174**, 135–149.
3 N. Q. Minh, *J. Am. Ceram. Soc.*, 1993, **76**, 563–588.
4 S. N. Truong, K. Van Pham, W. Yang and K. S. Min, *Proc. – 2016 IEEE Biomed. Circuits Syst. Conf. BioCAS 2016*, 2017, 456–459.
5 G. D. Wilk, R. M. Wallace and J. M. Anthony, *J. Appl. Phys.*, 2001, **89**, 5243–5275.
6 S. Kasamatsu, T. Tada and S. Watanabe, *Appl. Phys. Express*, 2009, **2**, 2–5.
7 O. I. Malyi, P. Wu, V. V. Kulish, K. Bai and Z. Chen, *Solid State Ionics*, 2012, **212**, 117–122.
8 P. Knauth and H. L. Tuller, *J. Am. Ceram. Soc.*, 2004, **85**, 1654–1680.
9 J. Maier, *Nat. Mater.*, 2005, **4**, 805–815.
10 J. Maier, *Chem. Mater.*, 2014, **26**, 348–360.
11 *Encyclopedia of Applied Electrochemistry*, ed. G. Kreysa, R. F. Savinell and K. Ota, Springer Science + Business Media, New York, 1st edn, 2014.
12 C. Korte, J. Keppner, A. Peters, N. Schichtel, H. Aydin and J. Janek, *Phys. Chem. Chem. Phys.*, 2014, **16**, 24575–24591.
13 G. F. Harrington, A. Cavallaro, D. W. McComb, S. J. Skinner and J. A. Kilner, *Phys. Chem. Chem. Phys.*, 2017, **19**, 14319–14336.
14 B. C. Steele and A. Heinzel, *Nature*, 2001, **414**, 345–352.
15 R. Pornprasertsuk, P. Ramanarayanan, C. B. Musgrave and F. B. Prinz, *J. Appl. Phys.*, DOI: 10.1063/1.2135889.
16 A. I. Ioffe, D. S. Rutman and S. V. Karpachov, *Electrochim. Acta*, 1978, **23**, 141–142.
17 S. Fabris, A. T. Paxton and M. W. Finnis, *Acta Mater.*, 2002, **50**, 5171–5178.
18 M. Raza, D. Cornil, J. Cornil, S. Lucas, R. Snyders and S. Konstantinidis, *Scr. Mater.*, 2016, **124**, 26–29.
19 H. Dixit, C. Beekman, C. M. Schlepütz, W. Siemons, Y. Yang, N. Senabulya, R. Clarke, M. Chi, H. M. Christen and V. R. Cooper, *Adv. Sci.*, 2015, **2**, 1500041.
20 S. Sanna, V. Esposito, J. W. Andreasen, J. Hjelm, W. Zhang, T. Kasama, S. B. Simonsen, M. Christensen, S. Linderoth and N. Pryds, *Nat. Mater.*, 2015, **14**, 1–5.
21 J. Pelleg, L. Z. Zevin, S. Lungo and N. Croitoru, *Thin Solid Films*, 1991, **197**, 117–128.
22 W. Liu, G. Ou, L. Yao, H. Nishijima and W. Pan, *Solid State Ionics*, 2017, **308**, 34–39.
23 S. Shukla and S. Seal, *Int. Mater. Rev.*, 2005, **50**, 45–64.
24 Y. Y. Wu and H. J. Keh, *J. Phys. Chem. B*, 2012, **116**, 3578–3586.
25 M. Raza, PhD thesis, University of Mons, 2017.
26 A. Faes, A. Hessler-Wyser, A. Zryd and J. Van Herle, *Membranes*, 2012, **2**, 585–664.
27 I. Kosacki, C. M. Rouleau, P. F. Becher, J. Bentley and D. H. Lowndes, *Solid State Ionics*, 2005, **176**, 1319–1326.
28 N. Sata, K. Eberman, K. Eberl and J. Maier, *Nature*, 2000, **408**, 946–949.

 This journal is © the Owner Societies 2018